



INVESTIGATION OF THE LATERAL RESPONSE OF FRICTION-BASED ISOLATORS UNDER MULTI-CYCLIC EXCITATIONS

M. Furinghetti⁽¹⁾, A. Pavese⁽²⁾

⁽¹⁾ PhD, Researcher, EUCENTRE (Pavia-Italy), marco.furinghetti@eucentre.it

⁽²⁾ Associate Professor, University of Pavia (Pavia-Italy), a.pavese@unipv.it

Abstract

The frictional response of Concave Surface Slider (CSS) devices has been more and more investigated both experimentally and numerically. These isolators have shown many advantages in comparison to the commonly used typologies of devices, such as lead rubber bearings or low and high damping rubber bearings: when implemented in structural systems, the eccentricity of the resultant base shear with respect to the center of mass is significantly reduced, since the lateral response of the devices is a direct function of the applied vertical force, i.e. the weight of the structure; furthermore new innovative sliding materials have been studied and implemented in real applications, in order to achieve high levels of energy dissipation, together with a high recentering capability, due to the geometry of the steel sliding surfaces. On the other hand, a number of issues about the behavior of friction-based isolators still have to be accurately analyzed. Among the others the distribution of the vertical load applied to the device is usually assumed constantly smeared on the sliding pad: however, recent research works have shown rather than constant distributions of contact pressure and this aspect is expected to cause variations in the commonly known dependency of the friction coefficient on the vertical load. Moreover, when a CSS device is subjected to long lasting dynamic excitations, the so called “cyclic effect” leads to a decay of the friction coefficient during time. Such a decay trend can be analyzed in terms of friction coefficient as a function of the cumulative dissipated energy, and can be fully described by an exponential equation, properly calibrated; the decay behavior is also supposed to be characterized by dependencies on both sliding velocity and contact pressure, i.e. vertical load. Then, a direct comparison between flat and concave sliding motions needs to be carried out, aiming at highlighting the differences in the frictional response of these typologies of movements.

In the present work the dynamic behavior of a friction based device has been deeply examined, thanks to the outcomes of a wide experimental campaign carried out at the EUCENTRE TREES Lab in Pavia on full scale flat and curved sliders, equipped with innovative sliding materials. Precisely, the cyclic effect caused on the friction coefficient by long lasting bi-directional dynamic motions has been characterized, by assuming several combination of sliding velocity and vertical load values. Moreover, the comparison among different diameters for the sliding pads in flat motions has been studied, in order to underline any “size effect” on the frictional response. Then, the comparison between flat and curved sliding motions has been carried out. Finally, such results have also been considered analytically, aiming at evaluating the consequences of the aforementioned features on the response of structural system base-isolated with CSS devices.

Keywords: friction coefficient, cyclic effect, sliding motion, cloverleaf orbit, heating phenomena.

1. Introduction

Concave Surface Slider devices represent an effective solution for base-isolation design problems. In such isolators the energy dissipation capability is induced by the sliding motions which occur at one or more sliding interfaces. The spherical shape of the sliding surfaces provides a significant recentering behavior, by means of the stepwise projection of the applied vertical load with respect to both horizontal directions. Several research studies and experimental assessments have been carried out in the past, for a comprehensive characterization of the lateral response of CSS devices: such investigations have led to a better understanding of the overall behavior of the isolators [4, 7, 9]. One of the most important assumptions states that the lateral response of a CSS device can be considered as the direct summation of the recentering force and the frictional force [2]: even though no direct comparison between the total force response of a curved slider and the individual numerical recentering force and experimental frictional response of a flat slider can be found in the literature, especially for full-scale devices, all the analytical models, which have been developed up to nowadays, follow this assumption. Furthermore, experimental results used for analytical model calibration are usually returned by uni-directional testing campaign; on the other hand, data about bi-directional tests on CSS devices are limited. Experimental campaign have shown a number of dependencies of the frictional response on some of the input parameters, such as the sliding velocity and the vertical load; a continuous degradation of the friction coefficient value has been also noticed when a long-lasting cyclic horizontal loading is applied [3, 8]. However, these influences have been found in uni-directional motions, whereas bi-directional responses still have to be properly investigated [6, 11].

In this work the outcomes of a wide three-dimensional experimental campaign have been analyzed, relative to full scale devices: precisely, both curved and flat sliding conditions have been considered, in order to provide a direct comparison between the lateral response of a DCSS device with the frictional force provided by the flat slider. Moreover, effects in the friction coefficient value due to different diameters of the sliding pad have been investigated, when subjected to flat sliding motions. Finally, an analytical expression for the computation of an average friction coefficient per cycle has been proposed, when a bi-directional cloverleaf orbit is assumed; such a procedure has allowed to underline the behavior of friction-based devices under long-lasting cyclic excitations.

2. Full-scale devices description

In the presented experimental campaign both uni-directional and bi-directional tests have been performed on ad hoc designed devices [5]. The former device consists of a Flat Slider (FS), which can accommodate bi-directional movements up to a vectorial value equal to 250mm (Fig. 1): such a Flat Slider consists of an upper flat sliding surface, a flat cylindrical slider together with its house. The upper flat stainless steel surface has been polished to mirror finish, in order to achieve a surface roughness index Ra equal to 0.2, whereas the slider and the relative house are built with S355JR steel. On top of the slider the sliding pad is installed.

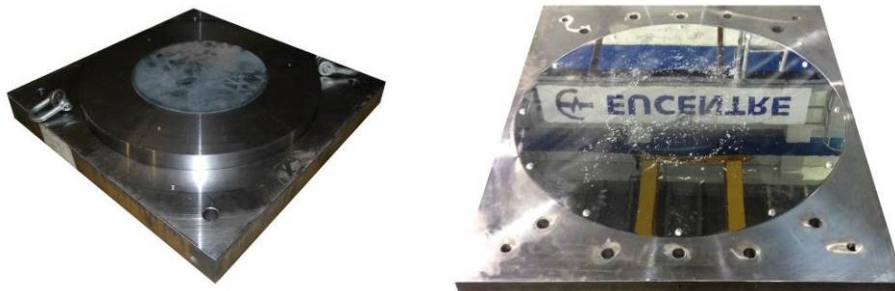


Fig. 1 – Flat Slider (FS) device: realized device

Three circular sliders have been designed, for testing sliding pads with different diameters (160mm, 260mm e 400mm): thanks to this setup it is possible to evaluate the size effect of the sliding pad on the force response, for given values of both sliding velocity and contact pressure.

The latter device is a DCSS device (Double Concave Surface Slider) with one internal non-articulated slider (Fig. 2): both the spherical sliding surfaces have the same radius of curvature and the internal slider houses two circular sliding pads, each one having a diameter equal to 260mm. Both the stainless steel curved sliding surfaces have been polished to mirror finish, in order to achieve a surface roughness index Ra equal to 0,2.



Fig. 2 – Double Concave Surface Slider (DCSS) device: realized device

Also this device accommodates bi-directional movements up to a total vectorial displacement equal to 250mm. Both the upper and lower sliding surfaces have a radius of curvature R equal to 1.6m and the non-articulated slider has a horizontal diameter of 260mm and a vertical height of 120mm, so that the equivalent radius of curvature is equal to 3,08m.

The Flat Slider has been equipped with three internal sliders: such sliders have different diameters, aiming at underlining the consequences of the “size effect” on the frictional response of the considered sliding materials; the realized diameters are 160mm, 260mm and 400mm. Concerning the Double Concave Surface Slider, one diameter equal to 260mm has been designed: this diameter value is included in the slider set of the FS device, in order to compare the flat sliding response to the curved one. In Fig. 3 the realized sliders are shown.

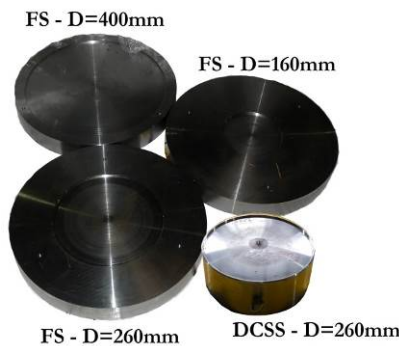


Fig. 3 – Realized flat and curved internal sliders

Two different sliding materials have been tested and studied. The former (Material A) consists of a graded Polytetrafluoroethylene (PTFE) filled with bronze fibers, with a solid lubricate; the latter (Material B) is a pigmented graded PTFE filled with carbon fibers, with a solid lubricate. Since Material B has carbon fibers in its formulation, the corresponding Young’s modulus is higher in comparison to Material A: this aspect is expected to cause differences in the cumulative damage during the testing protocols.

3. Testing protocols

In this section a description of the testing campaign is provided, which has been carried out at the EUCENTRE TREES Lab in Pavia, by means of the Bearing Tester System [10]; a special setup of the testing equipment has



been used, in order to perform three-dimensional tests on the previously shown devices [3]. Since both the spherical sliding surfaces of the DCSS device have the same radius of curvature, at both the sliding interfaces the same sliding movement (in opposite direction) occurs: however, the modulus of both displacement and velocity is half of the total displacement and velocity respectively. Thus, the testing protocol of the Flat Slider has been obtained from the protocol of the DCSS device, reducing of 50% both the displacement and velocity values. For each test the vertical load has been computed according to a selection of three contact pressure values (15MPa, 33MPa e 45MPa) and to the size of the considered sliding pad: for the DCSS the diameter of the sliding pad is equal to 260mm, whereas for the FS three different diameters have been studied (160mm, 260mm and 400mm). All the testing protocols have been performed on both the devices equipped with the aforementioned sliding materials.

3.1 Bi-axial testing protocol

Uni-directional tests have been carried out on the FS device with three different pad diameters, for a frictional characterization of the implemented materials, according to the common practice. Thus, the specimens have been subjected to sinusoidal displacement waveforms, with several combinations of peak velocity and applied vertical load. In Table 1 a summary of the uni-directional testing protocol is reported for the Flat Slider (FS).

Table 1 – Uni-directional testing protocol for FS device

Test #	Test Name	Max Displ. D [mm]	Max Velocity V [mm/s]	Contact pressure p [MPa]	Cycles [#]
1	Uni-directional	100	0.6	15	1
2	Uni-directional	100	50	15	3
3	Uni-directional	100	100	15	3
4	Uni-directional	100	200	15	3
5	Uni-directional	100	0.6	33	1
6	Uni-directional	100	50	33	3
7	Uni-directional	100	100	33	3
8	Uni-directional	100	200	33	3
9	Uni-directional	100	0.6	45	1
10	Uni-directional	100	50	45	3
11	Uni-directional	100	100	45	3
12	Uni-directional	100	200	45	3

3.2 Tri-axial testing protocol

Concerning the bi-directional testing protocol, a number of pairs sliding velocity-vertical load have been considered and the “cloverleaf” shape trajectory has been assumed, as ruled by the standard code of Anti-Seismic devices UNI:EN15129:2009 [1]. For each test the cloverleaf trajectory has been repeated twice, achieving a total number of lobes equal to 8: in this way the investigation of the cyclic effect under bi-axial excitation has been carried out, in terms of friction coefficient decay, as a function of the dissipated energy. A special resampling procedure has been applied, aiming at obtaining bi-directional orbits with a stepwise constant value of the tangent velocity modulus for the whole duration of the test [3]. In Fig. 4 the aforementioned test typologies are shown, for a fixed value of maximum velocity: the horizontal axis represents the time vector, normalized with respect to the duration $T_{O,max}$ of the Ordinary cloverleaf orbit test, whereas the vertical axis



contains the values of the modulus of the tangent velocity of the specimen, divided by the maximum velocity value of the test.

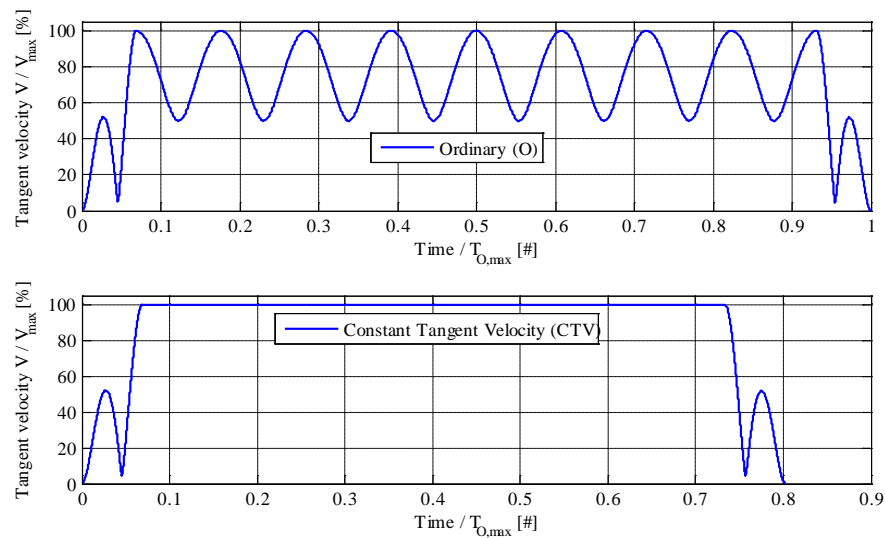


Fig. 4 – Constant Tangent Velocity (CTV) tests

As well as for the unidirectional testing protocol, the displacement signals for the FS device have been accordingly scaled by a factor equal to 50%. In Table 2 the summary of the bi-directional testing protocol for the DCSS device is reported.

Table 2 – Bi-directional testing protocol for DCSS device

Test #	Test Name	Max Displ. D [mm]	Max Velocity V [mm/s]	Contact pressure p [MPa]	Cycles [#]
1	Cloverleaf – CTV	0.200	0.020	15	2
2	Cloverleaf – CTV	0.200	0.080	15	2
3	Cloverleaf – CTV	0.200	0.300	15	2
4	Cloverleaf – CTV	0.200	0.020	33	2
5	Cloverleaf – CTV	0.200	0.080	33	2
6	Cloverleaf – CTV	0.200	0.200	33	2
7	Cloverleaf – CTV	0.200	0.300	33	2
8	Cloverleaf – CTV	0.200	0.020	45	2
9	Cloverleaf – CTV	0.200	0.080	45	2
10	Cloverleaf – CTV	0.200	0.300	45	2

4. Experimental results

The results of all the previously described testing protocols are hereby analyzed. Actually, the size effect related to the sliding pad diameter has been firstly investigated; then, a direct comparison between the responses under



curved rather than flat sliding conditions has been provided, and, finally, a new analytical expression for an average friction coefficient value per cycle has been proposed, by assuming a cloverleaf bi-directional orbit.

4.1 Size-effect on friction coefficient

In Fig. 5 and Figure Fig. 6 the dependency of the friction coefficient with respect to contact pressure is analyzed, for materials A and B respectively.

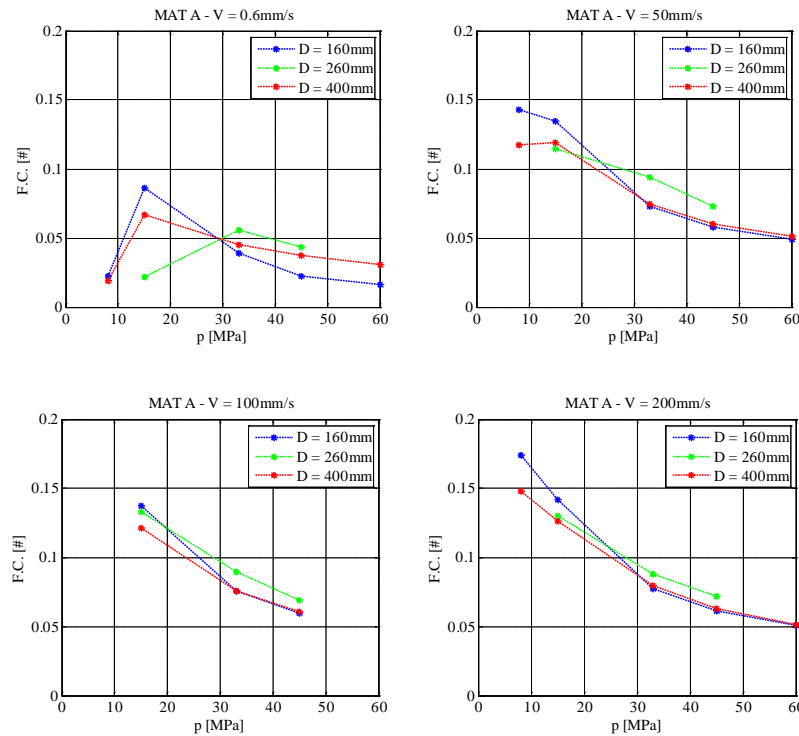
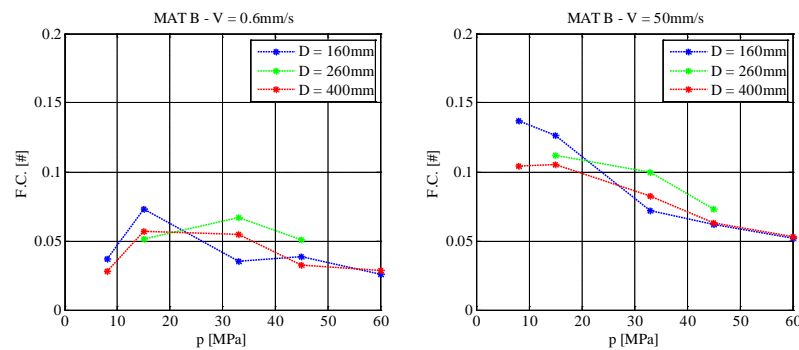


Fig. 5 – Flat Slider, size effect: friction coefficient vs. contact pressure, Material A



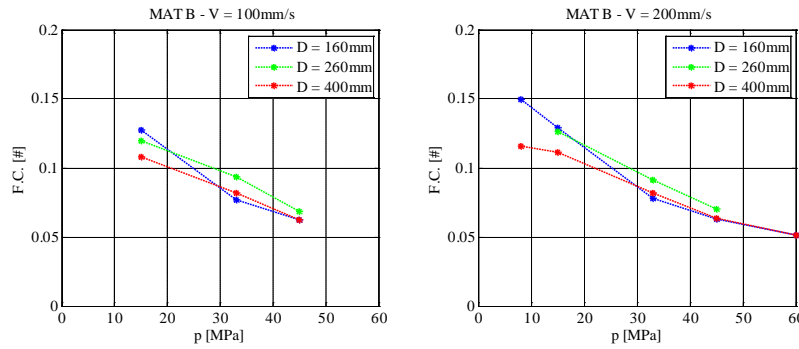


Fig. 6 – Flat Slider, size effect: friction coefficient vs. contact pressure, Material B

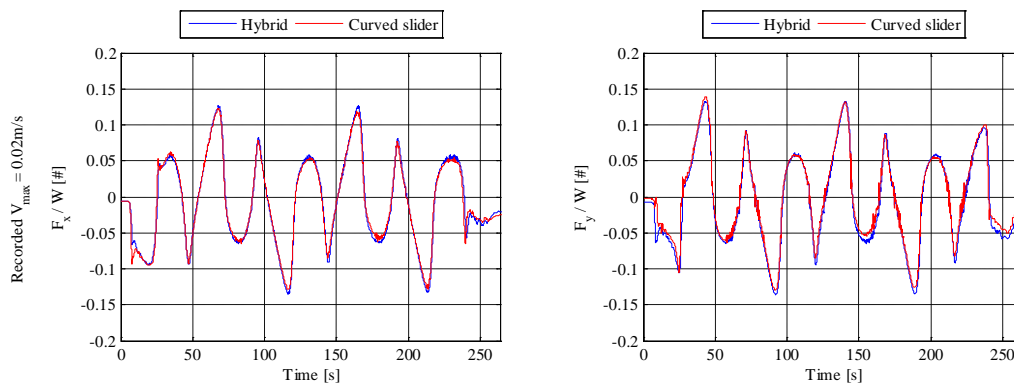
It can be noted that the “size effect” becomes negligible as the sliding velocity increases: for all the tested internal flat sliders, the frictional curves are almost overlapped at all the considered points. A more irregular behavior can be detected for the lowest velocity considered in the testing protocol (0.6mm/s), at which an unusual trend is found for low values of contact pressure. Such a phenomenon is mainly due to the irregular distribution of the vertical load applied to the sliding pad, when a low value of vertical load is considered. Same comments can be drawn by considering results of material B.

4.2 Comparison between flat and curved sliding motions

The comparison of the experimental lateral response of the DCSS device to a “hybrid force” signal has been analyzed. The hybrid force (eq. (1)) is computed as the summation of an experimental part, which consists of the frictional forces of the corresponding test performed on the Flat Slider, and a numerical part, that is represented by the analytical model of the restoring force (modelled as a linear spring with respect to displacement).

$$F_{Hybrid} = F_{f-Flat} + \frac{W}{R_{eq}} \begin{bmatrix} x \\ y \end{bmatrix} \quad (1)$$

In Fig. 7 and Fig. 8 results are shown for CTV cloverleaf tests, at the intermediate value of contact pressure (33 MPa), for both materials A and B: results are shown in terms of lateral force time histories along both x and y directions. It can be noted that the combination of the experimental force originated by the Flat Slider device and the numerical modelling of the restoring force provides a very good estimate of the lateral response of the DCSS isolator along both directions of motion, at all velocity levels and for both materials A and B. The same behavior has been noticed also for lower and higher contact pressure values.



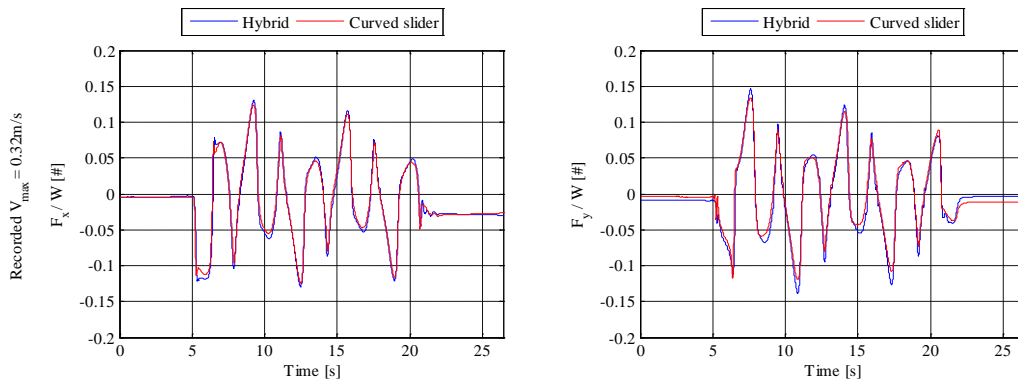


Fig. 7 – Hybrid vs. Experimental CTV orbits response (Material A – $p = 33\text{MPa}$)

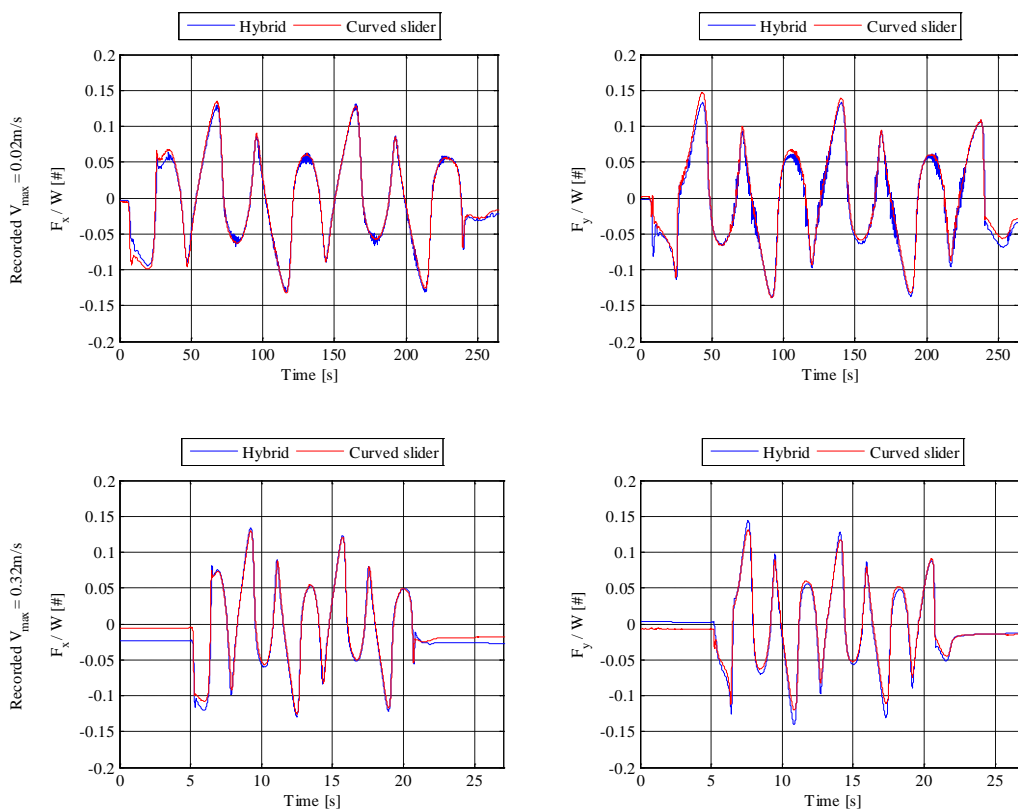


Fig. 8 – Hybrid vs. Experimental CTV orbits response (Material B – $p = 33\text{MPa}$)

This aspects could imply some changes in the standard code which rules the testing procedures of anti-seismic devices, such as UNI:EN15129:2009 [1]: for a full characterization of the frictional behavior of a DCSS device, the sliding pad only can be tested: however, particular attention has to be focused on the scaling factor to be applied to both maximum displacements and velocity, in order to properly describe the sliding motion.

4.3 Analytical computation of frictional properties

In the present work a new procedure has been defined, similarly to the one ruled by the code UNI:EN15129:2009 [1] for the computation of the friction coefficient as a function of the dissipated energy per cycle (EDC). In order to consider the same type of equation provided by the code, a “bi-directional cycle” has been defined for the cloverleaf orbit. For such a trajectory, one cycle can be considered as a set of two consecutive lobes (Fig. 9): in fact, when a uni-directional sinusoidal waveform is applied, the device in a single

cycle has to reach the maximum and the minimum displacements respectively starting from the centered position (the maximum value of the displacement is reached twice along two different directions); if two lobes of the cloverleaf trajectory are considered, the maximum vectorial displacement is reached twice along two different (and orthogonal) directions as well.

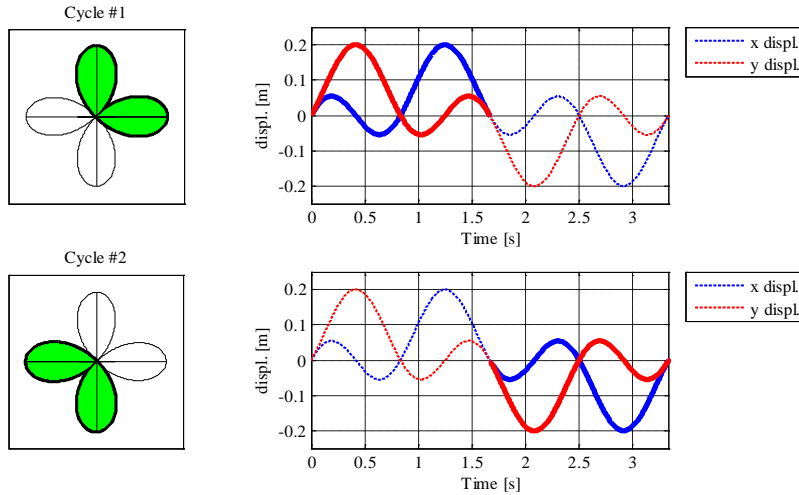


Fig. 9 – Definition of the bi-directional cycle with cloverleaf trajectory

Therefore for all the tests four full cycles can be analyzed, since the cloverleaf orbit has been repeated twice (8 lobes). According to the aforementioned definition, the average friction coefficient per cycle can be computed as the ratio between the energy dissipated per cycle (EDC) and the multiplication between the applied vertical load and the total length of the trajectory along two lobes (eq. (2) (3)).

$$\mu = \frac{EDC}{4,844 D_{\max} W} \quad (2)$$

In the case of a bi-axial motion, the energy dissipated per cycle EDC is computed as the total work, that is the integral of the scalar product between the force and the differential displacement vectors.

$$EDC = \int \vec{F} \cdot d\vec{s} \quad (3)$$

In the followings results for the friction coefficient decay of the CTV cloverleaf orbit for a number of combinations of sliding velocity and vertical load are shown. Concerning the instantaneous friction coefficient value, additional fluctuations can be generally detected with respect to the average trend: since results have been returned by CTV tests, the dependency of such fluctuations on the sliding velocity can be excluded (Fig. 10); consequently, more research has to be carried out on this aspect.

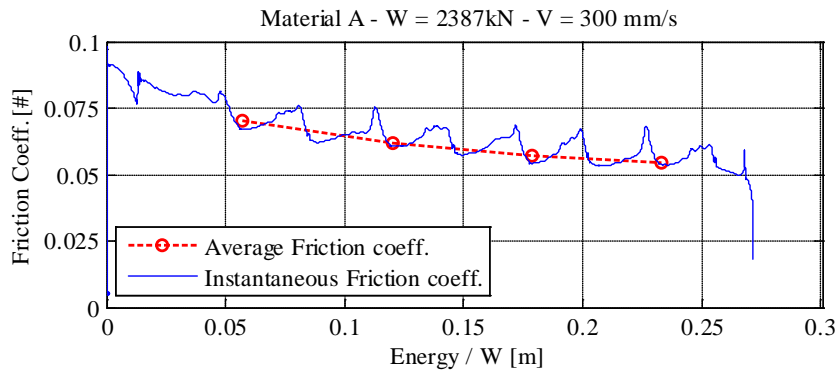


Fig. 10 – Average vs. Instantaneous friction coefficient

In Fig. 11 the cyclic effect on the DCSS isolator response is investigated for both materials A and B. The horizontal axis represents the cumulative dissipated energy, normalized with respect to the vertical load, whereas the y-axis reports the friction coefficient value, which is computed according to the aforementioned procedure.

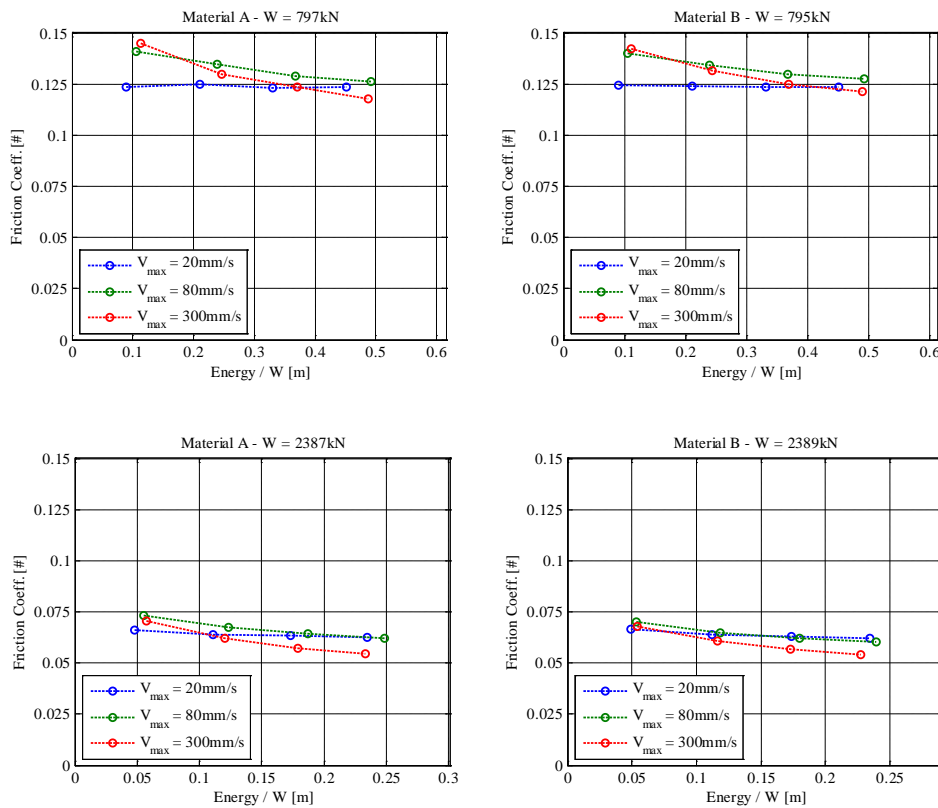


Fig. 11 – DCSS-D260: Friction coefficient decay behavior with cloverleaf CTV orbits

It is possible to note that for low values of sliding velocity and for the lowest contact pressure the friction coefficient decay is negligible, whereas it is more evident as the vertical load increases. On the other hand, for high value of sliding velocity, the friction coefficient decay is much more significant, for any level of contact pressure. The same behavior can be noticed for both the sliding materials A and B.

4.4 Wear evidences

In the followings the wear of the sliding pads at the end of the whole testing protocols is analyzed for both materials A and B. In Fig. 12 the wear status of the sliding pads FS-D260 relative to the flat slider device are shown.



Fig. 12 – Wear evidence – FS-D260 material A (left) and material B (right)

As can be noted, Material A is much more damaged in comparison to Material B: this could be due to the minor Young’s modulus of Material A, which is filled with bronze fibers, rather than Material B which is filled with carbon fibers; in fact, Material B shows limited wear evidences.

Finally, in Fig. 13 the wear of the sliding pads DCSS-D260 for both materials A and B are shown.



Fig. 13 – Wear evidence – DCSS-D260 material A (left) and material B (right)

In the case of DCSS device the sliding pads look less damaged: some small fragments are detected on the sliding surfaces in both cases; nonetheless, the overall shape of the pads looks undeformed. This can be due to a confinement effect which is provided by the curved sliding surface, so that a shear failure plane can not be originated (Fig. 14).

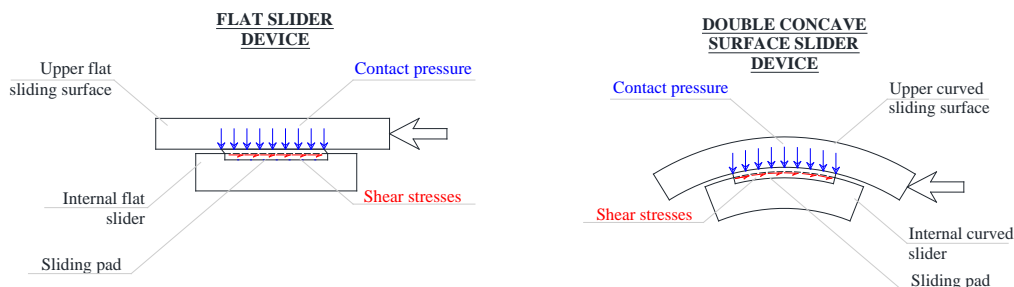


Fig. 14 – Wear evidence – Shear stresses during flat (left) and curved (right) sliding motions

As shown in the Fig. 14, for flat sliding motions the contact pressure is orthogonal with respect to the shear stresses, thus a shear failure is likely to occur. On the other hand, during curved sliding motions, the



components of the contact pressure which are parallel to the curved sliding surface provide an additional shear resistance to the sliding pad, which decreases the damage due to the sliding motion. Thus, a testing protocol carried out on a flat sliding pad represents the “worst condition” for the sliding material.

5. Conclusions

In this paper the experimental response of ad hoc realized full scale devices has been deeply analyzed, by means of a wide experimental campaign, carried out at the EUCENTRE TREES Lab in Pavia. All the designed devices have been equipped with innovative Teflon-based sliding materials, and different diameters of the sliding pads have been studied for flat sliding conditions. Special attention has been focused on the comparison of the frictional force due to curved rather than flat sliding motions, the investigation of the cyclic effect and the influences of the sliding pad diameter on the friction coefficient value.

The comparison between the flat frictional responses for all the studied materials among the considered diameters of the sliding pads has shown no significant differences from the friction coefficient value point of view. Thus, it can be assessed that the size effect seems to have a negligible influence on the friction coefficient value, for medium-to-high velocity and vertical load levels.

The cyclic effect generally leads to decreasing values of the friction coefficient with respect to the dissipated energy. Additional fluctuations of the friction coefficient are also detected with respect to the average trend, which do not depend on sliding velocity, since results have been returned by CTV tests. On the other hand, a complex dependency of the exponential trend shape on both sliding velocity and vertical load has been found: for low values of both velocity and vertical load the frictional decay is negligible, and increases as the velocity increases; at high values of vertical load, the cyclic degradation of friction becomes non negligible also for low values of velocity, and same behavior for higher velocities is detected.

The composition of the experimental frictional force of the flat slider and the numerical recentering force provides an excellent estimation of the lateral response of a DCSS device, for any condition of loading. Thanks to the proper scaling procedure of the flat testing protocol, the experimental flat frictional response returns same results which occur at both the curved sliding interfaces of the DCSS isolator. Thus, for both modelling identification and experimental characterization purposes, the response of a CSS device can be described by modelling numerically the restoring force with a linear spring and by characterizing the frictional response of the flat sliding pad, subjected to a properly scaled testing protocol.

It has also been noticed that flat sliding conditions leads to heavy wear evidences on the sliding material rather than curved sliding motions: thus, flat sliding motions represent the worst case for wear resistance investigations of sliding materials under dynamic loading.

6. Acknowledgments

Part of the current work has been carried out under the financial support Italian Civil Protection, within the framework of the Executive Project 2014–2016 (Project S2.0 – Seismic isolation and supplemental damping systems: evaluation of the seismic response of devices and structures). Authors reserve a special acknowledgment to Prof. Virginio Quaglini and Dr. Paolo Dubini, who have furnished the innovative sliding materials which have been tested, and have provided a fundamental technical support.

7. References

- [1] CEN (2009): Comité Européen de Normalisation TC 340, European Code UNI EN 15129:2009 Anti-seismic devices, European Committee for Standardization. Brussels, Belgium.
- [2] Furinghetti M, Casarotti C, Pavese A (2012): Effects of bi-directional motion on a structural system isolated with DCSS devices with laying defects. *15th WCEE, World Conference on Earthquake Engineering*, Lisbon, Portugal.



- [3] Furinghetti M, Casarotti C, Pavese A (2014): Bi-directional experimental response of full scale DCSS devices. *2ECEES, Second European Conference on Earthquake Engineering and Seismology*, Istanbul, Turkey.
- [4] Furinghetti M, Pavese A (2015): Numerical Assessment on the Seismic Response of a Base-Isolated Building under Bi-Directional Motion. *5th ECCOMAS Thematic Conference on Computational Methods in Structural Dynamics and Earthquake Engineering*, Crete Island, Greece, May 25-27.
- [5] Furinghetti M (2015): Assessment and Modelling of the Seismic Response of Curved Surface Slider devices under Multi-Axial Input. PhD thesis, UME School Pavia, Italy.
- [6] Gandelli E, Quaglini V, Dubini P, Bocciarelli M, Poggi C (2013): Frictional heating in sliding seismic isolators. *ANIDIS 2013 L'ingegneria sismica in Italia*, Padova, Italy.
- [7] Jangid RS (1997): Response of pure-friction sliding structures to bi-directional harmonic ground motion. *Engineering Structures*, **19** (2), 97-104.
- [8] Lomiento G, Bonessio N, Benzoni G (2013): Concave sliding isolator's performance under multi-directional excitation. *Ingegneria Sismica*, **30** (3), 17-32.
- [9] Lomiento G, Bonessio N, Benzoni G (2013): Friction Model for Sliding Bearings under Seismic Excitation. *Journal of Earthquake Engineering*, **17**, 1162-1191.
- [10] Peloso S, Pavese A, Casarotti C (2012): EUCENTRE TREES lab: Laboratory for training and research in earthquake engineering and seismology. *Geotechnical, Geological and Earthquake Engineering*, **20**, 65-81.
- [11] Quaglini V, Bocciarelli M, Gandelli E, Dubini P (2014): Numerical Assessment of Frictional Heating in Sliding Bearings for Seismic Isolation. *Journal of Earthquake Engineering*, **18** (8), 1198-1216.